



Spatiotemporal Analysis of Water Balance Components and Their Projected Changes in Near-future Under Climate Change Over Sina Basin, India

Saswata Nandi¹ · Janga Reddy Manne^{1,2} 

Received: 17 November 2019 / Accepted: 13 April 2020 /
Published online: 22 May 2020
© Springer Nature B.V. 2020, corrected publication 2020

Abstract

Quantification of water-budget components is an essential step in the planning and management of water resources in any river basin. Recently several studies emphasized that climate change would inevitably affect terrestrial hydrology. This study applies distributed hydrological modeling using the Variable Infiltration Capacity (VIC) model to simulate the water balance components in the Sina basin, a drought-prone region in India. We analyzed the long-term spatiotemporal dynamics of precipitation, evapotranspiration, surface runoff, and baseflow components, and their alterations due to impending climate change. The study employed the Mann-Kendall test and Sen's slope estimators to analyze the spatiotemporal trends of the water balance components during the baseline (1980–2010) and for the near future (2019–2040) periods. For the baseline period, precipitation exhibited an increasing trend, particularly during the monsoon season. On the evaluation of the annual water balance components, it showed that the basin has a low annual rainfall (~718 mm) and relatively a very high annual evapotranspiration (~572 mm) during 1980–2010, which might be the main reason for frequent droughts in the study basin. Further, for analyzing the climate change impacts on the water budget in the Sina basin, the VIC model was forced with outputs from a set of global climate models for near future (2019–2040) for two emission scenarios RCP4.5 and RCP8.5. Analysis of the results revealed that the water balance components in the near future would be negatively affected by climate change despite their increasing pattern in the baseline period. In comparison to the baseline (1980–2010), the surface runoff would decrease by as much as 32% for the near future, which stresses for planning and adaptation of appropriate mitigation measures in the basin.

Keywords Hydrological modeling · VIC model · Sina river basin · Water budgeting · Trend analysis · Climate change

Electronic supplementary material The online version of this article (<https://doi.org/10.1007/s11269-020-02551-2>) contains supplementary material, which is available to authorized users.

✉ Janga Reddy Manne
mjreddy@civil.iitb.ac.in

Extended author information available on the last page of the article

1 Introduction

Water resources management involves precise delineation and regulation of the water balance components at different spatiotemporal scales. Understanding of water budget and hydrologic processes of a catchment is critical for the planning and management of water resources in a basin. The terrestrial water balance is composed of precipitation, interception, infiltration, evapotranspiration, soil moisture, runoff, and groundwater flow. However, various components of water balance are often difficult to measure (e.g., soil moisture and evapotranspiration), which makes their quantification a quite challenging task (Sheffield et al. 2009; Meenu et al. 2013). Further, the spatiotemporal distribution of the water balance components is likely to be affected by the changes in the climatic conditions (Sivakumar 2011). To study the impact of climate change on the various water balance components, generally, Global Circulation Models (GCMs) are used with different climate scenarios.

Moreover, several studies have employed an ensemble modeling approach using multiple GCMs to predict the likely changes in future projections and reduce model uncertainty (Mehrotra et al. 2013). Therefore, the use of only one (or few GCMs) and raw GCM output is responsible for poor understanding of uncertainty in future projections and biased climate projection results. Coupled model inter-comparison project phase 5 (CMIP5) provides the output from the most recent GCMs for future climatic scenarios. However, a large number of parameterization and coarser-resolution GCMs make the GCM output biased and unsuitable for their application at the watershed level (Gosling et al. 2011). Therefore, bias-corrected and downscaled outputs from GCMs offer more accurate and finer resolution information for the climate change scenarios. In this direction, the newly released NASA's Earth Exchange Global Daily Downscaled Projections (NEX-GDPP) dataset, comprised of statistically downscaled output from 21 newer generation GCMs, has been applied in few regional studies and found to be effective in the reduction of uncertainty for near-term and long-term climate projections (Ahmadalipour et al. 2017; Bao and Wen 2017).

Hydrological models are helpful in quantitative understanding of various hydrological processes in a catchment, and their use in combination with downscaled climate models can be useful to study the variations of water balance components for the future scenarios (Yu et al. 2018). Therefore, these models are engaged in guiding the management actions, decision-making, and as well as for assessing the impact of climate change (Meenu et al. 2013). From a plethora of hydrological models, selecting one for application to a specific problem is crucial because of desired spatiotemporal resolution, allowable degree of error and uncertainty in the model simulations, availability of data, etc. (Bloschl and Sivapalan 1995). Improved processing of spatial information and computational resources has driven hydrologists to develop sophisticated physically-based distributed models (Liang et al. 1994). A distributed approach for hydrological modeling considers the spatial variability of the different hydrological processes in a catchment by grid wise distribution of the various model parameters, catchment characteristics (e.g., topography, soils, and vegetation cover), and meteorological forcings (e.g., precipitation), thereby being preferred over the lumped models (Beven 2010). The VIC model is one such physically based macroscale hydrological model, which comprises improved representation of horizontal resolution using sub-grid variability of soil moisture storage, land use, nonlinear representation of base-flow and inclusion of topography for better representation of orographic precipitation and environmental lapse rate (Liang et al. 1994). In the past, the VIC model was successfully used for hydrological simulations of varying catchment sizes and estimated the various hydrological processes satisfactorily (Liang et al.

1994). In the past, the calibration of the VIC model is majorly performed using manual calibration, which has a huge influence on the hydrological model performance. So, there is a greater need for developing effective procedures via automatic calibration of the VIC model. In recent studies, the self-adaptive differential evolutionary (SaDE) algorithm found to be yielding good results for optimization of complex water resources problems and performing better over the simple GA and DE algorithms in terms of computational efficiency and accuracy (Sirsant and Reddy 2018). Therefore this study proposes the SaDE method for automatic calibration of the VIC model.

Also, there were limited or no studies that have used distributed models for data-sparse regions in India like the Sina basin. The Sina river basin is one of the highly drought-prone areas of the Maharashtra State in India. Recent studies in the Sina basin also noted that although the total precipitation stayed almost constant in the last few decades, the spatiotemporal variation led to several severe droughts and worsening of the financial condition of the poor farmers (e.g., Udmale et al. 2014). Therefore, a better understanding of water resource availability and their changing pattern plays a key role in meeting the needs for sustainable development in the region. Also, there are no previous studies in the basin that have applied distributed modeling for assessing the climate change impacts at a finer resolution using an ensemble of multiple GCMs.

Considering the above issues, the primary objectives of this study are framed as (1) to estimate the regional water budget in the Sina river basin, (2) to analyze the spatial patterns and temporal trends for the water balance components, and (3) to assess the impact of climate change on the water balance components of the Sina basin. Such analysis will aid in providing sustenance for irrigation, food security, and the health of the river ecosystem.

The following sections contain a detailed description of the methods (Sect. 2), case study and data (Sect. 3), results and discussion (Sect. 4), and conclusions (Sect. 5) from this study.

2 Methodology

The present study adopted VIC based distributed hydrological modeling to simulate the water balance components in the river basin. Figure 1 shows an overview of the methodology adopted in the present study. First, the different gridded input data required for VIC modeling over the Sina basin are collected, processed, and prepared in the required format. Then, the configuration (e.g., resolution of model grids, the number of soil layers, etc.) of the VIC model is selected based on suggestions from past studies. The automatic calibration of the VIC model is performed using a self-adaptive DE (SaDE) algorithm (Sirsant and Reddy, 2018), and the calibrated VIC model is validated using different performance measures.

The VIC model with climatic forcing for baseline (1980–2010) and near-future (2019–2040) periods is used to simulate the various water balance components. Spatiotemporal analysis of water balance components is carried out using standard trend analysis methods like the Mann-Kendall test and Sen's slope estimators at monthly, seasonal, and annual timescales. Subsequently, it assessed the impacts of climate change for near-future on the water resources in the basin. Brief details of the methods adopted in the study are explained below.

2.1 VIC Hydrological Model

For hydrological modeling, this study adopted the three-layer VIC model, which is a grid-based macroscale hydrological model that considers the fundamental interaction between

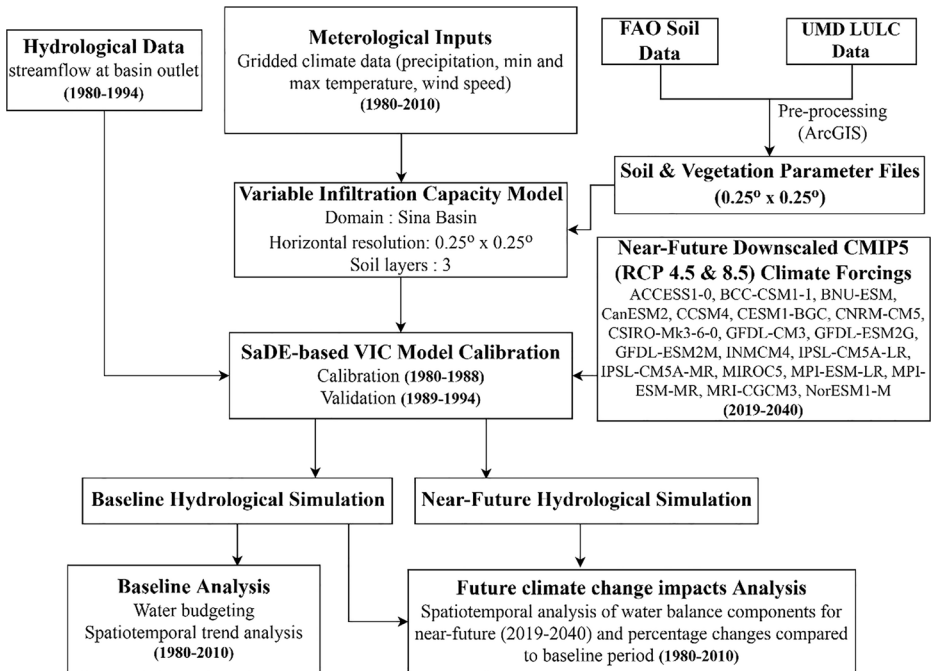


Fig. 1 Flowchart of the overall methodology used for VIC hydrological modelling and spatiotemporal analysis of water balance components in the Sina basin for baseline (1980–2010) and near-future (2019–2040) periods

vegetation, atmosphere, and soil water dynamics (Liang et al. 1994). The VIC model solves both the energy and the water balance components for each grid at daily or sub-daily time steps and is capable of representing the sub-grid heterogeneity in vegetation class, elevation, precipitation, and storage capacity of soil moisture in different soil layers. In this study, the Penman-Monteith method is selected for estimation of potential evapotranspiration, and the variable infiltration curve for separating the precipitation into direct runoff and infiltration in the VIC modeling environment. VIC model estimates the surface flow and baseflow separately. The top two soil layers contribute to the surface runoff, while the bottom soil layer contributes to the baseflow as per the ARNO formulation (Todini 1996). The water balance equation used in the VIC model is expressed as:

$$P = R + E + \frac{dS}{dt} \tag{1}$$

where P, R, E, and dS/dt are the precipitation, runoff, evapotranspiration, and changes in soil water storage, respectively.

2.2 Calibration of VIC Model Parameters

The performance of any hydrological model is predominantly affected by the calibration of model parameters, which may involve estimation of the unknown parameter values so that the model simulations can closely match with the observations of hydrological variables. The VIC model has several parameters; however, six parameters namely, infiltration parameter (b_{infil}), depth of three soil layers (d_1 , d_2 , and d_3), baseflow parameters (W_s and D_s), have a higher

influence on the model performance (Lohmann et al. 1998). The details of the model parameters and their ranges used for the calibration are presented in Table S1 (supplementary material).

In general, the manual calibration process, which involves a trial and error approach, was used for parameter estimation of the VIC distributed hydrological model. But this approach may require many hits-and-trials and finally may not guarantee an optimal parameter set. So, few studies used optimization methods like a genetic algorithm (Wang 1991), shuffled complex evolution algorithm (Vrugt et al. 2003), differential evolution (DE) (Qin et al. 2008), etc., for calibration of lumped and/or semi-distributed hydrological models. From recent studies, it was also noted that DE has specific advantages over other evolutionary methods, such as reliable, quick optimal solutions for complex problems and simplicity in implementation. Further, the self-adaptive version of DE (called SaDE), which offers more flexibility and avoids manual tuning of the parameters of the DE algorithm, and also provides high reliability in optimal solutions (Sirsant and Reddy, 2018). Therefore, the present study adopts a self-adaptive DE (SaDE) with Nash–Sutcliffe Efficiency (*NSE*) as the objective function. More details of SaDE based methodology for calibration of the VIC model are given in Appendix-1 (Supplementary Material).

The study utilizes standard performance measures such as coefficient of determination (R^2), Nash–Sutcliffe Efficiency (*NSE*), Percent of Bias (*PBIAS*), and Index of Agreement (*IoA*) to evaluate the performance of the VIC model. Brief details of the performance measures are given in Appendix-2 (Supplementary Material).

2.3 Trend Analysis Methods

Trend analysis is helpful to understand any significant changes in the various water balance components of the basin. This study uses Sen's slope method (Sen 1968) for estimating the trend magnitude and non-parametric Mann–Kendall test (Mann 1945, Kendall 1975, Adarsh and Janga Reddy 2015) to detect the presence of any significant trend in water balance components. Brief details of the Sen's slope method and Mann–Kendall test are given in Appendix-3 (Supplementary Material).

3 Case Study

3.1 Study Area

The Sina basin, one of the major feeder to the Bhima River, is selected as the study area. The basin falls in the state of Maharashtra, India with latitude $17^{\circ}29'N - 19^{\circ}15'N$ and longitude $74^{\circ}28'E - 76^{\circ}7'E$. The area of the basin is around 12,160 Km², and the length of the river is 180 km. The elevation varies from 561 m to 766 m in the basin. The study area has a semi-arid climate and is one of the frequent drought-prone areas of Maharashtra State. The economy of the people in the region is largely dependent on agriculture. Figure 2 shows the location map of the study area, modeling grids, and the outlet of the Sina river basin located near Wadakbal station. The average annual rainfall in the region is 718 mm. The mean daily maximum temperature ranges from 28.5° C to 39.1° C (in May), while the mean daily minimum temperature varies between 11.7° C to 23.0° C. Overall, the humidity is low in the region, and during summer, the average relative humidity can fall below 45%. Also, the rainfall over

the region is highly seasonal (i.e., monsoon season contributes over 80% of annual rainfall), and the impacts of climate change can be vital, which necessitates a thorough assessment of water balance components in the region. The Sina basin has no substantial flow control structure, which makes it an ideal case study for deriving general inferences on hydrological alterations due to climate change.

3.2 Data Used

VIC hydrological modeling is performed at a spatial resolution of $0.25^\circ \times 0.25^\circ$. Daily data of precipitation and temperature were acquired from Indian Meteorological Department (IMD) at a spatial resolution of $0.25^\circ \times 0.25^\circ$ and $1^\circ \times 1^\circ$ respectively. The wind speed data obtained from NCEP (National Centre for Environmental Prediction) reanalysis data at $2.5^\circ \times 2.5^\circ$ scale; Soil data acquired from FAO (Food and Agricultural Organization) harmonized world soil database at 30 arc-second (~ 1 km) spatial resolution; AVHRR (Advanced Very High-Resolution Radiometer) global land cover map obtained from the University of Maryland ($1 \text{ km} \times 1 \text{ km}$); SRTM (90 m) DEM collected from NRSC (National Remote Sensing Centre of India). The observed daily discharge data for the Wadakbal gauge station (basin outlet) was obtained from the WRIS-India (Water Resources Information System of India).

The data for near-future (2019–2040) climatic projections of precipitation, maximum and minimum air temperatures are obtained from 19 downscaled GCMs at a daily time scale, and at a spatial resolution of $0.25^\circ \times 0.25^\circ$ from NASA's NEX-GDDP dataset. A statistical downscaling algorithm, namely Bias-Correction Spatial Disaggregation (BCSD) method, was employed to generate the NEX-GDDP dataset (Thrasher et al. 2012). The 19 selected GCMs used in this study (from CMIP5 project) include ACCESS1-0, BCC-CSM1-1, BNU-ESM, CanESM2, CCSM4, CESM1-BGC, CNRM-CM5, CSIRO-Mk3-6-0, GFDL-CM3, GFDL-ESM2G, GFDL-ESM2M, INMCM4, IPSL-CM5A-LR, IPSL-CM5A-MR, MIROC5, MPI-ESM-LR, MPI-ESM-MR, MRI-CGCM3, and NorESM1-M. Brief details of these GCMs are given in Table S1 (Supplementary Material) and more information can be found from NEX-GDDP (<https://cds.nccs.nasa.gov/nex-gddp/>) hosted by NASA. This study uses the datasets of two climate projection experiments (i.e., Representative Concentration Pathways RCP 4.5 and RCP 8.5) obtained from NEX-GDDP to assess the climate change impacts on water budget components of the basin.

4 Results and Discussions

For the application of the VIC model, the catchment is divided into 27 grids of 0.25° spatial resolution. The grid-based VIC model simulates the time series of fluxes, viz., surface runoff, baseflow, evapotranspiration, etc. A standalone routing scheme is employed in this study to transfer the runoff resulted from the individual grid to the outlet of the basin.

4.1 Model Calibration and Validation

The SaDE is used for automatic calibration of the VIC hydrological model and calibrated using the observed discharge data collected at Wadakbal station, which is the outlet of the Sina basin. The VIC model is calibrated using the observed data from 1980 to 1988, and validation is carried out for the period 1989–1994. The final calibrated values of the six parameters of the

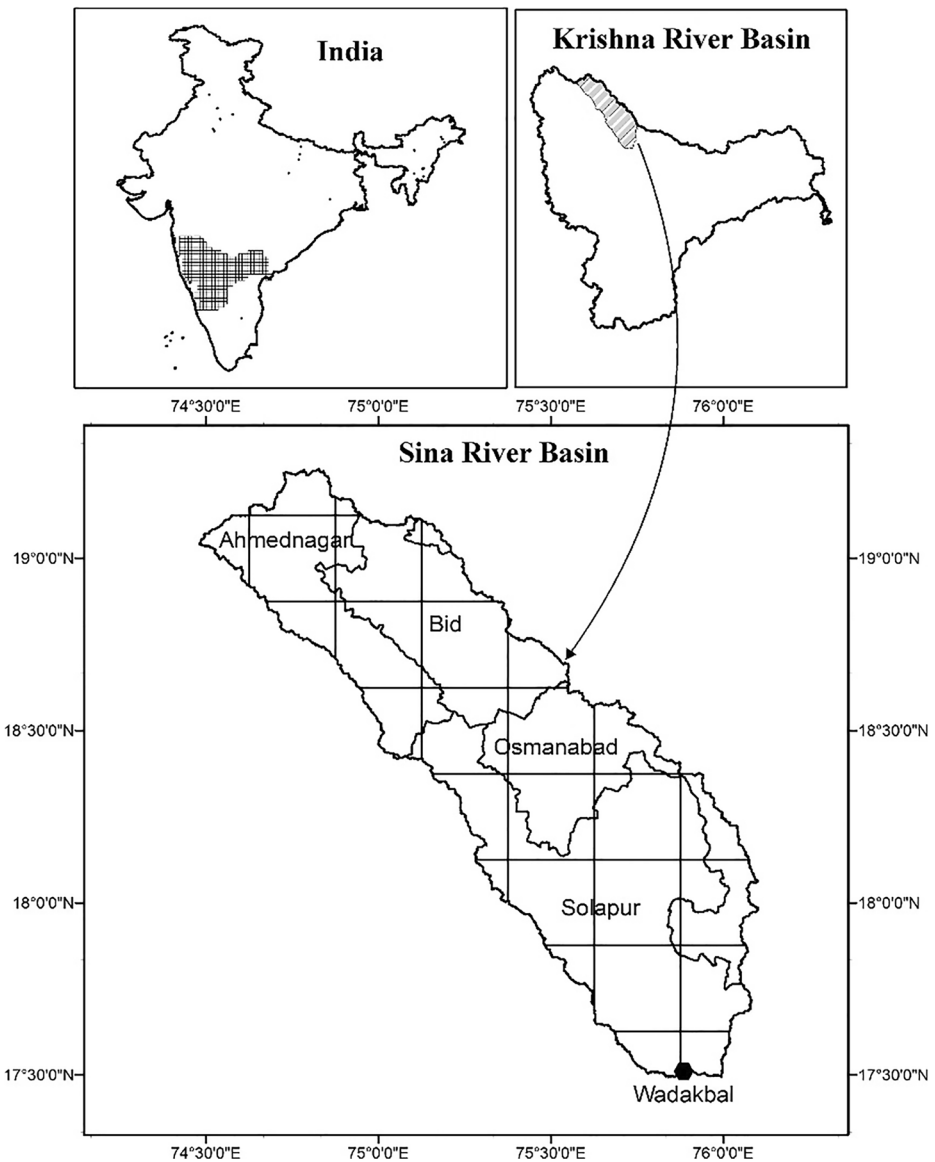


Fig. 2 Location map of the study area

VIC model are $b_{inflt}=0.06$, $D_s=0.01$, $W_s=0.99$, $d_1=0.2$, $d_2=1.31$, and $d_3=0.92$. Figure 3 shows the comparison between simulated and observed monthly flows at the basin outlet, during both the calibration and validation phases. An excellent agreement is found between the simulated and observed flows (including the peaks) during both calibration and validation phases. The performance measures viz., R^2 , NSE , $PBIAS$, and IoA are found to be respectively 0.91, 0.95, 12, and 0.98 for the calibration period; and 0.88, 0.94, 18, and 0.98 for the validation period. There are no universally agreed to threshold values for the model performance evaluation. However, past studies noted that satisfactory model performance can be

realized if the values of $R^2 > 0.6$, $NSE > 0.5$, $PBIAS < \pm 20\%$, and $IoA > 0.75$ (Moriassi et al. 2015). Thus, the model performs excellently with respect to all the performance measures during the calibration as well as the validation periods, and thus used for further analysis.

4.2 Water Balance Analysis for the Sina River Basin

The VIC model inputted with observed daily meteorological forcing for the baseline period (1980–2010) to simulate the daily water balance components viz., precipitation, evapotranspiration, surface runoff, and baseflow. Firstly, basin-wise analysis of the water balance components performed at monthly, seasonal, and yearly time scales for the baseline period (1980–2010) (Table 1). Also, annual average values of water-balance components are computed in a grid-wise manner and used for spatial analysis.

4.2.1 Basin-wise Water Budgeting

The results of the monthly water balance components obtained over the Sina basin are presented in Table 1. The monthly average precipitation increases from March to September and then decreases from October to February in the basin. From Table 1, it can be observed that streams in the basin are supported by depleting soil water storage (i.e., negative dS) for the period of October–May, while during remaining periods of the year, the basin experiences a natural recharge (i.e., positive dS) in its soil water storage. Maximum positive water storage in the basin is found in September, whereas the largest negative water storage is estimated in the month of March. On average, the evapotranspiration is higher than the precipitation for six months, i.e., from December to May. Also, evapotranspiration is found to be the major component in the water balance of the Sina basin. Such high evapotranspiration over the basin might have contributed to the decreased soil moisture and subsequent water scarcity and drought conditions in the districts of Ahmednagar, Bid, Osmanabad, and Solapur in the Sina basin.

For the seasonal water balance study, the water year (i.e., 1 June to 31 May) is categorized into four seasons: monsoon season (JJAS), the autumn season (ON), winter season (DJF), and summer season (MAM). The results of the seasonal water balance of the Sina river basin,

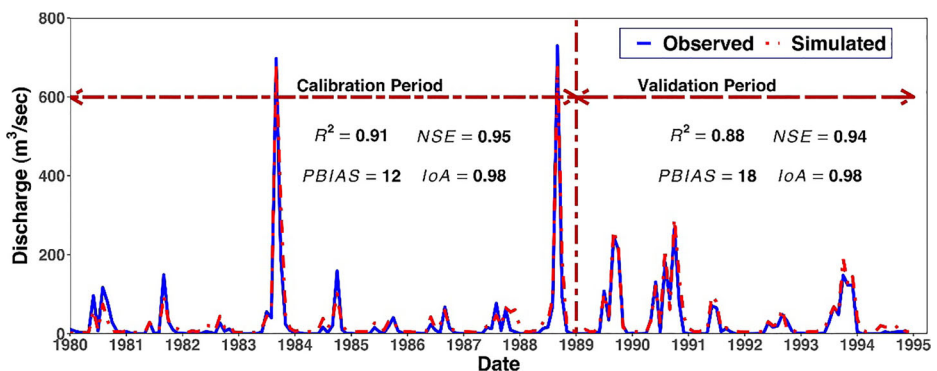


Fig. 3 Performance comparison of observed and simulated streamflows from VIC model at monthly scale during calibration (1980–1988) and validation period (1989–1994). The R^2 , NSE , $PBIAS$, and IoA are used to assess the performance of the VIC model simulation during calibration and validation period

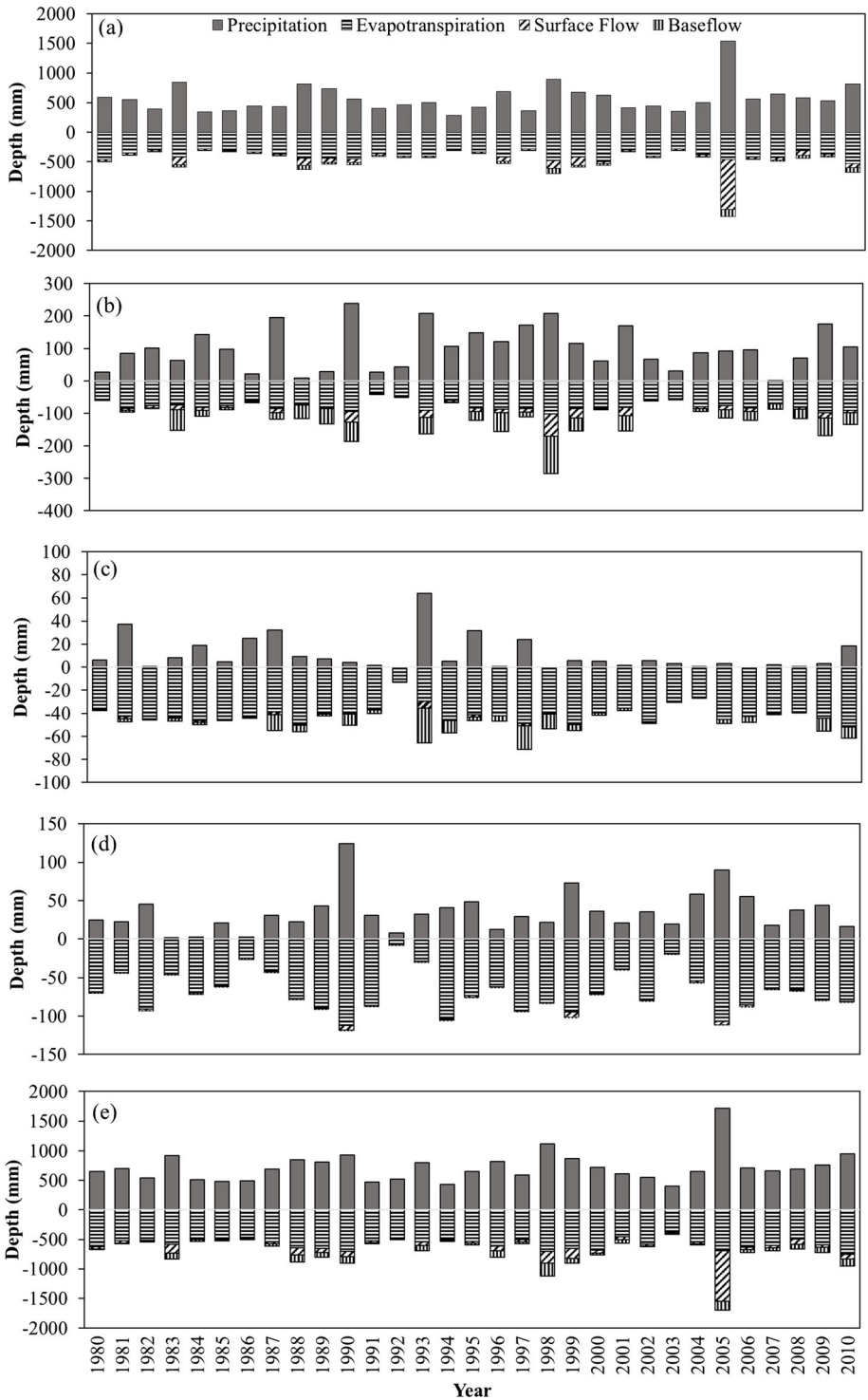
Table 1 Mean statistics of different components of simulated water balance components in the Sina river basin for different temporal scales (monthly, seasonal, and annual) during 1980–2010. The seasonal and annual trend statistics of Mann-Kendall Z-value and Sen's slope estimator values for the four primary water balance components are given in the parentheses (the two comma-separated values).

Month/ Season	Precipitation (mm)	Evapo- transpiration (mm)	Surface flow (mm)	Base flow (mm)	Total Runoff (mm)	Runoff Coefficient (%)
Monthly scale						
Jan	3.46	13.66	0.22	1.16	1.38	39.88
Feb	1.27	14.97	0.07	0.38	0.45	35.43
Mar	5.17	19.21	0.27	0.17	0.44	8.51
Apr	7.25	20.54	0.34	0.08	0.42	5.80
May	21.96	28.01	1.05	0.10	1.15	5.24
Jun	128.74	87.22	10.13	1.57	11.7	9.09
Jul	120.07	102.75	14.85	3.08	17.93	14.93
Aug	137.51	99.08	15.99	4.96	20.47	14.90
Sep	186.37	97.31	28.30	14.95	43.25	23.21
Oct	82.24	61.20	9.86	19.46	29.32	35.65
Nov	18.26	15.95	1.31	6.87	8.18	44.79
Dec	5.92	11.96	0.46	3.89	4.35	73.48
Seasonal scale						
Monsoon	572.69 (1.05, 4.25)	386.36 (0.98, 1.4)	69.27 (1.19, 0.41)	24.56 (2.14, 0.56)	93.83	16.38
Autumn	100.50 (0.58, 0.69)	77.15 (1.05, 0.24)	11.17 (0.71, 0.07)	26.33 (1.26, 0.45)	37.50	37.30
Winter	10.65 (-2.26, -0.25)	40.59 (-0.24, -0.03)	0.74 (-2.09, -0.02)	5.42 (0.65, 0.04)	6.16	57.84
Summer	34.37 (1.50, 0.65)	67.72 (0.75, 0.42)	1.67 (1.53, 0.04)	0.34 (1.87, 0.01)	2.01	5.84
Annual scale						
Annual	718.22 (1.12, 4.65)	571.85 (1.26, 2.40)	82.84 (1.25, 0.54)	56.64 (2.04, 1.64)	139.48	19.42

The bold values indicate statistical significance at 5% significance level for MK tests ('+sign' for increasing and '-sign' for decreasing trend)

comprising different water balance components, are presented in Table 1 and graphically in Fig. 4. It can be noticed that about 80% (572.7 mm) of annual rainfall (718.2 mm) received in the monsoon season. The annual total runoff (surface flow + baseflow) of the basin is 139.5 mm, mainly contributed by the Monsoon season 93.8 mm (67%), of which 24.5 mm (26%) comes from the baseflow contribution. The total runoff of 93.8 mm has resulted from the monsoon precipitation of 572.7 mm, which has caused a low runoff coefficient (0.16) for the basin, very similar to the results reported by Biggs et al. (2007). This may be due to the high evapotranspiration in the basin and low rainfall spells during the season. The evapotranspiration is estimated to be 386.3 mm, which is 68% of the yearly evapotranspiration. For monsoon season, the change in storage (dS) is estimated as 92.5 mm, which indicates positive water balance, which may lead to the natural replenishment of groundwater storage.

From the results of water balance analysis for the autumn season (Table 1), it is noticed that the season has an average rainfall of 100.5 mm, out of which 37% (37.5 mm) converts into the



◀ **Fig. 4** Results of VIC model simulations for water balance components during different seasons of (a) monsoon, (b) autumn, (c) winter, (d) summer, and (e) annual scale in the Sina basin during 1980–2010

runoff. It is interesting to note that in spite of getting only 13% of monsoon precipitation, the autumn produces an almost equal amount of baseflow to that of the monsoon season. It signifies the fact that for the autumn season, streamflow is supplemented mostly by stored soil water and groundwater, which get replenished by the high precipitation in the watershed during the monsoon season. In the autumn season, the change in storage (dS) is found to be -14.15 mm, which indicates that there are negative water balance and subsequent depletion of groundwater during this season. From Table 1 and Fig. 4c-d, it can be noticed that the rainfall is relatively very less in winter and summer seasons (with the average rainfall of 10.65 mm and 34.37 mm, respectively). The runoff in winter and summer is 6.16 and 2.01 mm, respectively, which are less than 5% of the average yearly runoff. Baseflow in winter and summer seasons are quite low compared to the other two seasons. The average evapotranspiration is higher than the mean precipitation during winter and summer seasons, which also resulted in a negative change in storage (-36.1 mm for winter, and -35.36 mm for summer season) in the basin. The basin entirely depends on rainfall (no snow-melt runoff in the basin). Therefore, the rabi crops have heavily impacted by such a water deficit situation in the basin. The river basin produces more than two-thirds of the total annual runoff during the monsoon season and generates almost no runoff in the summer and winter. Therefore, unless proper storage structures are constructed in the basin (to store the water during monsoon season), drought conditions may prevail during the other seasons of the year. It should be noted that several past studies also reported drought conditions in this region (Suryawanshi and Gaikwad 1984).

Figure 4e shows the results of the annual water balance components during 1980–2010. The figure shows that there exist notable periodicities of 5–8 years in the various water balance components. For example, the years 1984, 1990, 1998, and 2005 were very wet, while the years 1986, 1994 and 2003 were very dry. The average annual rainfall in the basin for 1980–2010 is estimated at 718.2 mm (Table 1), which is much lower than India's average annual rainfall of 1190 mm. The average annual surface runoff in the basin is 82.8 mm, while the average annual baseflow is 56.6 mm. Therefore, the baseflow is contributing about 40% of the total runoff in the Sina river basin. From Table 1, it can be noticed that the average annual rainfall of 718.2 mm resulted in only 139.48 mm of total runoff in the study area. This led to a low runoff coefficient of 0.19 in the basin, which was also highlighted by past studies conducted on the basin (Biggs et al. 2007). The annual average evapotranspiration from the study area is 571.8 mm. The lower runoff coefficient in the basin is attributed to the high evapotranspiration rate and low rainfall in the basin. Appropriate planning may help in the utilization of this runoff effectively for various needs of the basin. From Table 1, it can also be noticed that the water balance components are closely balanced for the study area.

4.2.2 Basin-wise Temporal Trend Analysis

Table 1 also presents the results of MK statistics and Sen's slope estimator values for basin-wise seasonal and annual trends for the four water balance components during the baseline period (1980–2010). On an annual basis, for the whole catchment, it is noticed that there is an increasing trend for precipitation (4.6 mm yr^{-1}), evapotranspiration (2.40 mm yr^{-1}), surface runoff (0.54 mm yr^{-1}), and baseflow (1.64 mm yr^{-1}). However, the Mann-Kendall test

performed at 5% significance level revealed that only the trend in the baseflow component is statistically significant and the trends for other water balance components (i.e., precipitation, evapotranspiration, and surface flow) are not statistically significant ($p > 0.05$). The increasing trend of precipitation in the basin is in agreement with the results reported by Guhathakurta and Saji (2013) and possibly caused by the climatic changes. The rate of increase in evapotranspiration might be attributed to the different factors like land use/land cover changes, the creation of smaller reservoirs, newer irrigation schemes, and increased radioactive forcing and temperature. As the increasing trend of evapotranspiration might counteract the increasing trend of precipitation, the response of runoff to increased precipitation in the basin is likely to be more uncertain. During 1980–2010, there is a significant increase in the baseflow, while the change in surface runoff remains insignificant, indicating a shift in their contribution to the streamflow.

From the seasonal analysis, precipitation shows a positive trend ($p > 0.05$) in most of the seasons except winter, where a significant negative trend is identified over the basin. Evapotranspiration also showed a positive trend ($p > 0.05$) during monsoon, autumn, and summer seasons; and a negative trend ($p > 0.05$) during the winter season. The increase in monsoon rainfall resulted in an increasing trend ($p > 0.05$) of surface runoff in the monsoon. It can also be seen from Table 1 that the decreasing or increasing trend of surface runoff is similar to that of precipitation in all four seasons. The baseflow results displayed an increasing trend in all the seasons, though statistically significant ($p < 0.05$) only during the monsoon season. It is interesting to note that there is an increasing trend of seasonal baseflow for the winter season, even though the winter season exhibited a significant decrease in seasonal precipitation (Table 1). It indicates that the contribution of antecedent soil water storage to the baseflow plays an important role, especially during periods of little or no precipitation.

4.2.3 Fine Resolution Spatial Analysis of Water Balance Components

Fine resolution spatio-temporal trend analysis is carried out to analyze the spatial patterns in different water balance components at annual and seasonal time scales over the basin during 1980–2010 (Fig. 5). It can be seen from Fig. 5 that the water balance components are vastly varied across the study area. The variation of average annual precipitation and evapotranspiration ranging from 615 to 900 mm and 500 to 650 mm, respectively, across the catchment grids, with higher values on western parts than that of the eastern parts. The surface flow varies across the catchment with the annual average value ranging between 35 to 273 mm (the annual average value of whole Sina basin was 82.8 mm), indicating that the different grids of the study area have diverse runoff generation capacity because of the different soil type, land use, topography, geology, and river network characteristics. Such investigation also illustrates the benefits of a distributed hydrological modeling approach to represent spatially heterogenous water balance components in a river basin, which could not have been possible by using lumped hydrological models.

For trends in water balance components, annual total precipitation exhibited a distinctive regional pattern and has witnessed a significant increasing trend in the upstream area (or northern part) of the Sina River basin. The change in annual evapotranspiration is similar to that of the annual precipitation, which shows a significant increasing trend for few grids in the middle of the basin. The annual baseflow exhibits a positive trend all over the basin, with a significant increasing trend in the northern region of the study area. The spatial distribution of seasonal trends in precipitation, evapotranspiration, surface flow, and baseflow for monsoon

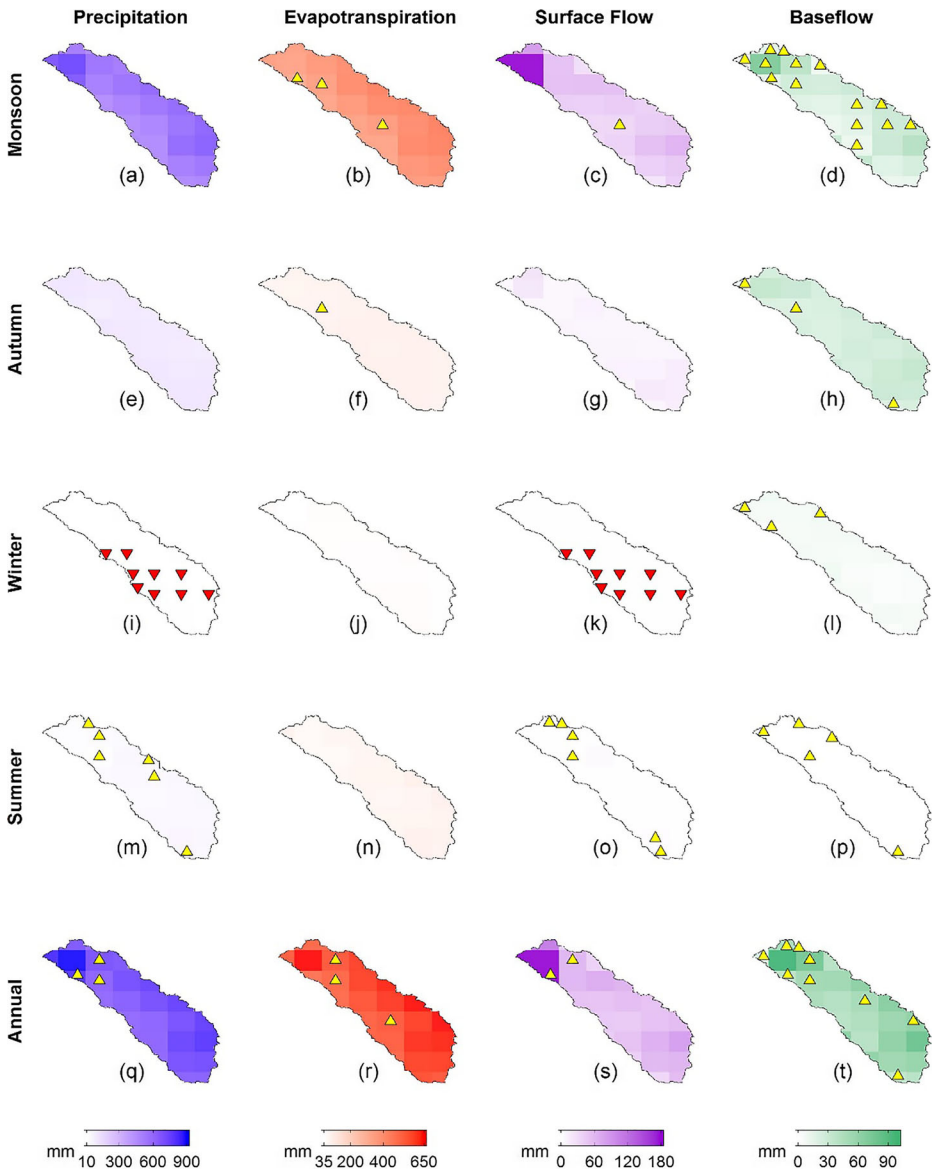


Fig. 5 Spatial variation of water balance components of precipitation(first column), evapotranspiration (Second column), surface runoff (third column), and baseflow (fourth column) in different seasons of monsoon (a-d), autumn (e-h), winter(i-l), summer (m-p), and annual (q-t) in near-future (2019–2040) over Sina basin. Up (down) triangles represents positive (negative) trend at 5% significance level

(Fig. 5a-d) are similar to those of the annual ones (Fig. 5q-t). The increasing or decreasing trend of autumn water balance components is not significant. Winter is the only season during which the precipitation and surface flow show a significant decreasing trend over different parts of the basin. The seasonal trend of winter evapotranspiration is also found to be decreasing but not statistically significant. The seasonal water balance components during summer show an increasing trend in the basin. The baseflow is the only water balance

component, which shows an increasing trend in all the seasons. The spatial distribution of seasonal trends in different water balance components shows an overall increasing trend except for winter, indicating a drier winter condition.

4.3 Impact of Climate Change On the Water Budget of the Sina River Basin

To assess the impact of climate change on the water balance components in the study area, the VIC model is forced with meteorological variables from 19 GCMs for two future climate projections (RCP4.5 and RCP8.5) for the near future (2019–2040). Figure 6a–h shows the projected monthly water balance components of the Sina basin for the near future (2019–2040), where dotted lines represent the ensemble mean, and shaded area represents the range of projections of all the 19 GCM projections.

For the RCP 4.5 projection, a decrease in rainfall is observed for the monsoon (3.02%), winter (87.41%), and summer (8.04%), while an increase in autumn rainfall by 2% is expected to follow. The maximum decrease in rainfall occurs in June, while October experiences an increase in rainfall by 7%, suggesting a possible temporal shift in the monsoon precipitation in near-future. Figure 6 also shows a decrease in the monthly evapotranspiration during the summer, winter, and autumn seasons. However, it is interesting to note that an increase in monthly evapotranspiration is expected during the monsoon season despite the overall decrease in monsoon precipitation. The increase in average daily temperature ($\sim 2^\circ\text{C}$) compared to the baseline might be a significant factor for such increasing evapotranspiration. The overall decrease in the monsoon precipitation and the increase in monsoon evapotranspiration lead to a negative impact on the surface runoff during the monsoon season, which is noticeable from Fig. 6. The summer and winter surface runoff are also expected to decrease in near-future, while surface runoff during autumn is predicted to experience a small increase due to the higher autumn precipitation. Although an overall decrease in the various monthly water balance components is expected to take place in the RCP4.5 scenario, the monthly baseflow is most likely to increase in the majority of the months (nine out of the twelve months). From Fig. 6, it can be noted that the baseflow in the basin typically shows a different trend from the precipitation (except for the monsoon), indicating that variation in monthly baseflow may not be directly associated with the variation in precipitation for the study area. The monthly water balance estimates for the RCP8.5 scenario are also shown in Fig. 6, which is found to be more or less similar to that of the RCP 4.5 scenario in the study region. In comparison with the RCP4.5, the surface runoff is found to be associated with a more distinct change for the RCP8.5 scenario, which signifies the high sensitivity of surface runoff to climate change.

Figure 6i shows the percentage changes in the annual water balance components for the near future about the baseline period, which indicates that most of the annual average water balance components decreasing in near-future for both the RCP4.5 and RCP8.5 scenarios. The average annual rainfall in the Sina river basin will be decreased by 3.8% and 2.7% (ensemble mean) for RCP4.5 and RCP8.5 scenarios, respectively. The annual evapotranspiration relative to the base period (1980–2010) has not shown much change in either of the RCP scenarios despite the relative decrease in the annual precipitation. It might be attributed to the increase in the daily temperature during the 2019–2040 period. For RCP4.5, the average daily maximum and minimum air temperature during 2019–2040 is expected to increase by 1.97°C and 1.87°C compared to the baseline period. The average daily maximum and minimum air temperature will increase by 2.11°C and 2.15°C , respectively, for the RCP8.5 scenario. This relatively high annual evapotranspiration and the decrease in annual precipitation will result

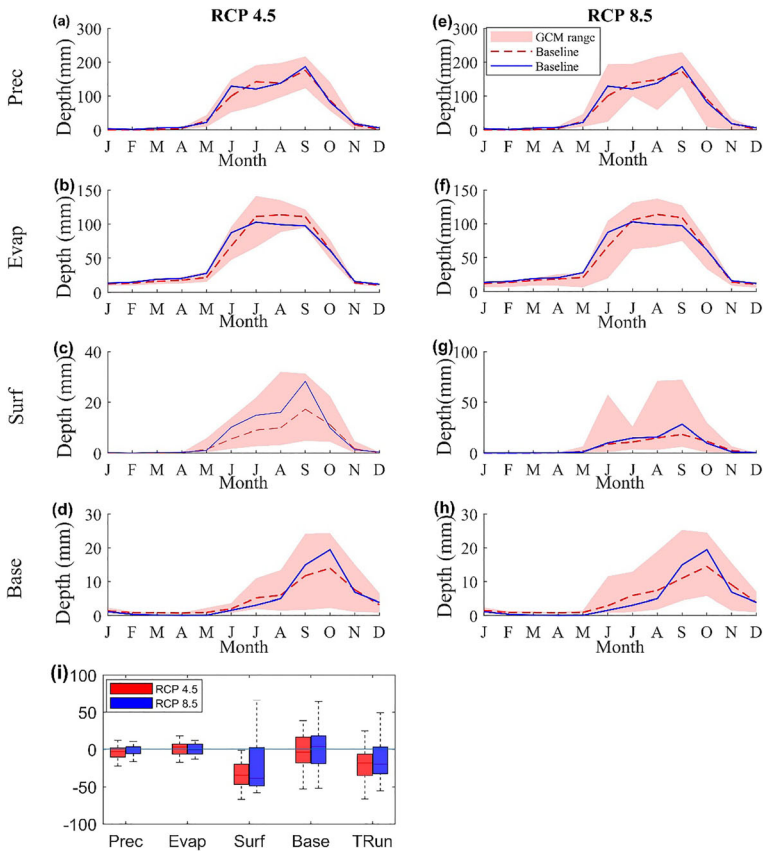


Fig. 6 Monthly variation (a–h) and percentage changes in annual water balance components (i) obtained using 19 GCMs. Rows (1), (2) (3) and (4) show monthly variation of: Prec (precipitation), Evap (evapotranspiration), Surf (surface flow), and Base (baseflow) for near-future (2019–2040). The first and second column for the first four rows shows the variation of monthly water balance components under RCP 4.5 and RCP 8.5 scenarios, respectively. The percentage changes in annual water balance components of Prec, Evap, Surf, Base and TRun (total runoff) in near-future (2019–2040) under RCP 4.5 and 8.5 scenarios is shown in (i), where the percentage changes are computed for 19 GCMs with respect to the baseline period (1980–2010)

in a decrease in the average annual total runoff, which can be seen from Fig. 6i. It is also interesting to note that the ensemble average annual surface flow is projected to decrease by 31.9% and 15.9% from the baseline under RCP4.5 and RCP8.5 scenarios, which indicates that the annual surface runoff is most sensitive to climate change than any other annual water balance components.

This study also assessed the spatial variations of annual and seasonal water balance components for the Sina basin. The analysis is based on the ensemble average of all the 19 GCMs. Figure 7 shows the spatial distribution of percentage changes in the seasonal and annual water balance components for RCP4.5 in near-future (2019–2040) as compared to baseline (1980–2010). The projected changes in the water balance components are not uniformly distributed over the study area, as some parts of the basin will experience a positive change in the various hydrological components while the other parts to face a negative change. From Fig. 7, it can be seen that mostly the various water

balance components in the upper part of the Sina basin may decrease in near-future, whereas a noticeable increase in the lower basin area. Among the various components, the surface flow and baseflow are expected to undergo the highest variation in terms of both positive and negative changes. The changes in surface flow are generally in agreement with the changes in precipitation for all the seasons. The magnitudes of seasonal change in the water balance components are mostly higher than that of their annual changes. Out of the four seasons, winter and summer are expected to experience the highest percentage changes. Figure 7p shows that the summer baseflow will face the highest percentage change in the near future. However, it is worth mentioning that this change is not very significant as the percentage change is very sensitive to the baseline value, which is extremely low (0.34 mm) in the case of summer baseflow. The projected changes in various water balance components for RCP8.5 scenario is quite similar to that of RCP4.5 and presented in Fig. S1. As compared to RCP4.5, water balance components in the RCP 8.5 will get slightly wetter during monsoon and autumn seasons and drier during winter and summer seasons.

4.4 Discussion

The novelty of the study includes: (1) application of the distributed hydrological model for water balance studies over the data-sparse Sina basin; (2) application of SaDE based methodology for effective calibration of the VIC model parameters; (3) applying the VIC model for assessing the climate change impacts at a finer resolution using an ensemble of multiple GCMs in the basin.

This study offered key insights into the quantitative assessment of water balance components of the Sina river basin at different spatiotemporal scales. The seasonal patterns of water balance components can have a substantial effect on agriculture and ecological sustainability in the study area. The results of the study infer that improved regional assessment of spatially complex water balance components is possible by using the VIC model in support of global datasets and limited local data. The study also infers that in the near future, the climate change would negatively affect the water balance in the Sina basin, particularly in Ahmednagar and Bid districts of the Maharashtra state; and the hydrological model driven by climate model forcing can be helpful to characterize such future changes. Therefore, it may be sensible to consider future hydro-climatic projections for the assessments of water availability and develop appropriate climate change mitigation measures for water resources management in the river basin.

5 Summary and Conclusions

This study employed the VIC hydrological model to simulate the water balance components for historical as well as for near-future periods under climate change scenarios in the Sina river basin and investigated the spatiotemporal patterns of water balance components. The parameters of the VIC model are estimated using SaDE method, and the model performance is evaluated using standard performance measures. Further, the water balance components for the Sina river basin were simulated and analyzed for baseline (1980–2010) and near-future (2019–2040) periods.

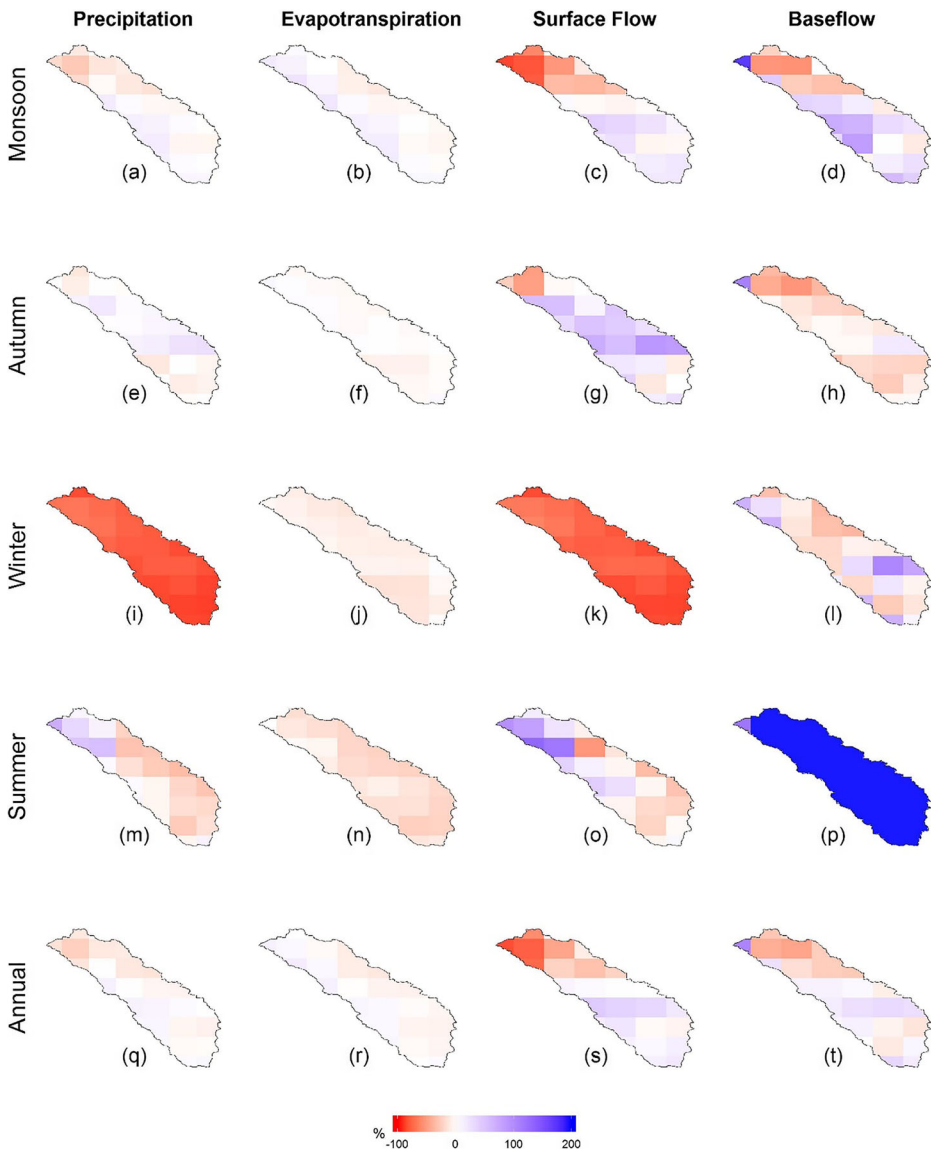


Fig. 7 The spatial distribution of percentage changes in water balance components of precipitation (first column), evapotranspiration (Second column), surface runoff (third column), and baseflow (Fourth column) in different seasons of monsoon (a–d), autumn (e–h), winter(i–l), summer (m–p), and annual (q–t) in the near-future (2019–2040). Here the percentage change has computed from the ensemble mean value obtained from 19 GCMs under RCP 8.5 scenario with respect to the mean of the baseline period (1980–2010)

The main conclusions drawn from the results of the study are:

- The VIC model, a distributed hydrological model, with application of SaDE based automatic calibration, found to be giving good performance for simulation of water balance components for river basins located in a semi-arid climate with limited data.

- The study area is receiving quite low annual rainfall (~718 mm) as compared to the annual average rainfall (~1190 mm) of India, and a major portion (~572 mm) of it lost in the form of evapotranspiration. Such low rainfall and high evapotranspiration might be the main contributing factors for frequent droughts in the Sina basin.
- The analysis of future water balance components indicated that projected climate change scenarios would negatively affect the water budget of the Sina basin. There may be an overall decrease in most of the water balance components in comparison to the baseline period. Furthermore, the precipitation during dry seasons is expected to decrease significantly under both RCP4.5 and RCP8.5 scenarios, which will substantially impact the other water balance components. Therefore, the study concludes that climate change will worsen the drought situation in the Sina basin.
- The annual surface runoff was found to be most sensitive to climate change as compared to other water balance components, and it is projected to decrease by 31.9% and 15.9% from the baseline period under RCP4.5 and RCP8.5 scenarios respectively. These changes in future water availability stress for developing appropriate climate change mitigation measures in the basin.

Acknowledgment Authors would like to thank the various agencies for funding support and providing the datasets: Department of Science & Technology (SPLICE–Climate Change Programme), Govt. of India, Project #DST/CCP/CoE/140/2018 for the funding support; the University of Maryland for NEX-GDPP dataset, IMD for precipitation and temperature dataset, NASA for NEX-GDDP dataset and others for providing or enabling access to the gridded datasets used in the study.

References

- Adarsh S, Janga Reddy M (2015) Trend analysis of rainfall in four meteorological subdivisions of southern India using nonparametric methods and discrete wavelet transforms. *Int J Climatol* 35:1107–1124
- Ahmadalipour A, Moradkhani H, Svoboda M (2017) Centennial drought outlook over the CONUS using NASA-NEX downscaled climate ensemble. *Int J Climatol* 37:2477–2491
- Bao Y, Wen X (2017) Projection of China's near- and long-term climate in a new high-resolution daily downscaled dataset NEX-GDDP. *J Meteorol Res* 31:236–249
- Beven K (2010) *Rainfall-runoff modelling: the primer*. Wiley, Chichester
- Biggs TW, Gaur A, Scott C, Thenkabail PS, Rao PG, Gumma MK, Acharya S, Turrall HN (2007) Closing of the Krishna Basin: Irrigation, streamflow depletion and macroscale hydrology. IWMI. <http://re.indiaenvironmentportal.org.in/files/RR111.pdf>
- Blöschl G, Sivapalan M (1995) Scale issues in hydrological modelling: A review. *Hydrol Process* 9(3–4):251–290
- Gosling SN, Taylor RG, Arnell NW, Todd MC (2011) A comparative analysis of projected impacts of climate change on river runoff from global and catchment-scale hydrological models. *Hydrol Earth Syst Sci* 15(1): 279–294
- Guhathakurta P, Saji E (2013) Detecting changes in rainfall pattern and seasonality index vis-à-vis increasing water scarcity in Maharashtra. *J Earth Syst Sci* 122:639–649
- Kendall MG (1975) *Rank Correlation Methods*, 4th edn. Charles Griffin, London
- Liang X, Lettenmaier DP, Wood EF, Burges SJ (1994) A simple hydrologically based model of land surface water and energy fluxes for general circulation models. *J Geophys Res* 99:14415–14428
- Lohmann D, Raschke E, Nijssen B, Lettenmaier DP (1998) Regional scale hydrology: II. Application of the VIC-2L model to the Weser River, Germany. *Hydrol Sci J* 43:143–158
- Mann HB (1945) Non-parametric tests against trend. *Econometrica* 13:163–171
- Meenu R, Rehana S, Mujumdar PP (2013) Assessment of hydrologic impacts of climate change in Tunga-Bhadra river basin, India with HEC-HMS and SDSM. *Hydrol Process* 27:1572–1589
- Mehrotra R, Sharma A, Kumar DN, Reshmidevi TV (2013) Assessing future rainfall projections using multiple GCMS and a multi-site stochastic downscaling model. *J Hydrol* 488:84–100

- Moriasi DN, Gitau MW, Pai N, Daggupati P (2015) Hydrologic and water quality models: Performance measures and evaluation criteria. *Trans ASABE* 58(6):1763–1785
- Qin AK, Huang VL, Suganthan PN (2008) Differential evolution algorithm with strategy adaptation for global numerical optimization. *IEEE Trans Evol Comput* 13(2):398–417
- Sen PK (1968) Estimates of the Regression Coefficient Based on Kendall's Tau. *J Am Stat Assoc* 63:1379–1389
- Sheffield J, Ferguson CR, Troy TJ, Wood EF, McCabe MF (2009) Closing the terrestrial water budget from satellite remote sensing. *Geophys Res Lett* 21:432–458
- Sirsant S, Reddy MJ (2018) Reliability-based design of water distribution networks using self-adaptive differential evolution algorithm. *ISH J of Hydraulic Eng* 24(2):198–212
- Sivakumar B (2011) Global climate change and its impacts on water resources planning and management: assessment and challenges. *Stoch Environ Res Risk Assess* 25(4):583–600
- Suryawanshi S, Gaikwad N (1984) An analysis of yield gap in rabi jowar in drought-prone area of Ahmednagar District. *Agric Situat India* 39:147–153
- Thrasher B, Maurer EP, McKellar C, Duffy PB (2012) Technical Note: Bias correcting climate model simulated daily temperature extremes with quantile mapping. *Hydrol Earth Syst Sci* 16:3309–3331
- Todini E (1996) The ARNO rainfall-runoff model. *J Hydrol* 175:339–382
- Udmale P, Ichikawa Y, Manandhar S, Manandhar S, Ishidaira H, Kiem AS (2014) Farmers' perception of drought impacts, local adaptation and administrative mitigation measures in Maharashtra State, India. *Int J Disaster Risk Reduct* 10:250–269
- Vrugt JA, Gupta HV, Bouten W, Sorooshian S (2003) A shuffled complex evolution metropolis algorithm for optimization and uncertainty assessment of hydrologic model parameters. *Water Resour Res* 39(8). <https://doi.org/10.1029/2002WR001642>
- Wang QJ (1991) The genetic algorithm and its application to calibrating conceptual rainfall-runoff models. *Water Resour Res* 27(9):2467–2471
- Yu Z, Gu H, Wang J, Xia J, Lu B (2018) Effect of projected climate change on the hydrological regime of the Yangtze River Basin China. *Stoch Environ Res Risk Assess* 32(1):1–16

Publisher's Note Springer Nature remains neutral with regard to jurisdictional claims in published maps and institutional affiliations.

Affiliations

Saswata Nandi¹ · Janga Reddy Manne^{1,2}

¹ Department of Civil Engineering, Indian Institute of Technology Bombay, Mumbai 400076, India

² Interdisciplinary Programme in Climate Studies, Indian Institute of Technology Bombay, Mumbai, India